applied sciences

MDPI

Article

Laboratory Investigation of the Mechanical Properties of a Rubber–Calcareous Sand Mixture: The Effect of Rubber Content

Xin Liu [1,*], Chaoyang Tian [1] and Hengxing Lan [1,2,*]

[1] Department of Geological Engineering, School of Geological Engineering and Geomatics, Chang'an University, Xi'an 710054, China; 2018126099@chd.edu.cn

[2] LREIS, Institute of Geographic Sciences and Natural Resources Research, Chinese Academy of Sciences, Beijing 100864, China

* Correspondence: xliu67@chd.edu.cn (X.L.); lanhx@igsnrr.ac.cn (H.L.); Tel.: +86-18591786872

Received: 28 July 2020; Accepted: 14 September 2020; Published: 21 September 2020

Abstract: This paper introduces a rubber–calcareous sand mixture as a lightweight building material in offshore engineering. The mechanical properties of mixtures of varying rubber contents were investigated by performing a one-dimensional (1-D) compression test in a modified oedometer cell, as well as a resonant column test. A discussion on the test results, along with detailed interpretations regarding the role of rubber chips in the mixtures, are provided. It was found that the virgin compression curves of the rubber–calcareous sand mixtures tended to converge at a certain stress level, whilst the stress level depended on the rubber content. Moreover, the relative breakage was examined by comparing the particle size distribution curves of the calcareous sand before and after the compression test. It was shown that the grain crushing of calcareous sand was less remarkable with the inclusion of rubber chips. Furthermore, the small strain shear modulus (G_0) of the mixtures decreased with the rubber content, yet the modulus reduction and damping curves exhibited little difference for the specimens of varying rubber contents.

Keywords: rubber–calcareous sand mixture; rubber content; compression; grain crushing; small strain shear modulus

1. Introduction

Calcareous sediments characterized by unique grain morphology are widely distributed near coral reefs [1]. They are commonly adopted as a building material in offshore engineering, ranging from conventional geotechnical applications (e.g., foundations, embankments, and retaining walls) to offshore hydrocarbon industries [2–5]. Understanding the engineering properties of calcareous sand is therefore of great importance. Over recent decades, the mechanical properties of calcareous sand have received global focus at both the academic and the practical levels. Across several studies, grain crushing under heavy loads was recognized as the major problem for calcareous sands, which is often associated with a loss of soil strength and the occurrence of ground deformation [6,7]. Wei et al. [8] conducted ring shear tests on calcareous sands under different levels of loading stress, and the formation of a shear band, along with the evolution of particle breakage, were examined. Donohue et al. [9] performed a series of cyclic loading tests on samples of Dog's Bay carbonate sand, and the development of volumetric strain due to grain crushing was explained based on the micromechanics at the grain contact level using numerical simulations. Moreover, a detailed summary of recent advances on grain crushing was also given by Xiao et al. [10]. Despite increased research efforts, most attempts in previous studies focus on quantitative descriptions of the crushability of grains, whereas measures to mitigate the effects of grain crushing for calcareous sands are rather limited.

As far as the weakness of the grain contacts of calcareous sands as compared to quartz sands is concerned, much evidence has shown that an admixture of rubber chips in sands from recycled scrap tires is useful for absorbing the energy at grain contacts, in particular, under dynamic loads [11,12]. As a matter of fact, the number of disposed tires in China exceeds 50 million per year [13], and thus there is a very large stock of rubber particles from recycled tires. As a type of lightweight material, an admixture of rubber with soils has been adopted in recent engineering applications, yielding satisfactory performance. In particular, as a backfill material, rubber soil can effectively improve the bearing capacity of foundations [14–16]. Moreover, as a hydrophobic material, rubber virtually does not react with underground water, hence the adverse impact on the environment is small [11]. However, previous research in this regard mainly uses quartz sand as the base sand. A question arises herein as to whether rubber chips can be adopted to effectively mitigate the adverse effects of grain crushing in calcareous sands.

With the aim of addressing the above concerns, a systematic laboratory program was carried out using rubber–calcareous sand mixtures with different rubber contents. Both a one-dimensional oedometer and a resonant column apparatus were adopted in this study, thus affording an explicit view on various engineering performances (i.e., grain crushing behavior and modulus reduction) of rubber–calcareous sand mixtures. The outcomes of this study will not only provide convincing evidence on the role of rubber chips in a mixture, but can also serve as a useful reference for engineering applications of rubber–calcareous sand mixtures in offshore engineering and for relevant theoretical developments.

2. Experimentation

2.1. Test Materials

In this study, to remove any possible influence of particle size and grading [17–20], sieved calcareous sand (300–425 μm) was adopted as the base sand, and rubber chips with the same range of particle sizes were used as the additive. To produce a sequence of rubber–sand mixtures, the quantity of rubber chips was varied from 0% to 10% by mass. For consistency, in the following sections, the numbers in the parentheses are used to denote the rubber content in the mixtures. As an example, the "sieved (5)" means sieved calcareous sand mixed with 5% of rubber chips, and the "sieved (0)" stands for pure calcareous sand. Calcareous sand originates from broken coral reefs, transported by the sea water. A careful examination using energy dispersive spectroscopy (EDS) indicated that the calcareous sands used in this study were composed primarily of calcium oxide. Micro-scale images of the test materials using a scanning electron microscope (SEM) are presented in Figure 1. Several unique features of the calcareous sand (Figure 1a) at the micro-scale level can be recognized, including the irregular particle shape (i.e., high angularity and low sphericity) and the presence of intraparticle voids, which could potentially result in a high void ratio for the calcareous sand [21–23]. On the other hand, the rubber chips (Figure 1b) were mainly composed of natural rubber. As seen in this Figure, some particles were prone to agglomerate and also to yield irregular particle shapes.

2.2. Sample Preparation and Test Methods

A series of one-dimensional (1-D) compression tests and resonant column tests were conducted on the rubber–calcareous sand mixtures. In the sample preparation, a certain amount of the calcareous sand and rubber chips were weighed in proportion. Then, the samples were thoroughly mixed. Note that the different specific gravities ($G_{s,\,calcareous}$ = 2.76; $G_{s,\,rubber}$ = 1.1) of the test materials were properly taken into account to determine the void ratio, as specified in the following equations:

$$e = \frac{G_{sRS} \cdot \pi D^2 H}{4 \cdot M} - 1 \quad (1)$$

$$G_{sRS} = \frac{G_{sR} \cdot G_{sS} RC}{RC(G_{\mathrm{sR}} - RC \cdot G_{\mathrm{sR}} + RC \cdot G_{\mathrm{sS}})} \tag{2}$$

$$RC = \frac{M_R}{M_R + M_S} \tag{3}$$

where G_{sRS} is the specific gravity of the binary mixtures; RC is the rubber content in percentage; M is the total mass, which is the sum of the calcareous sand (M_{S}) and rubber (M_{R}); D and H are the diameter and the height of specimen, respectively. To achieve a target void ratio, the specimens were created by successive light compactions. All tests were carried out under dry conditions, and no particle segregation was visible during the test.

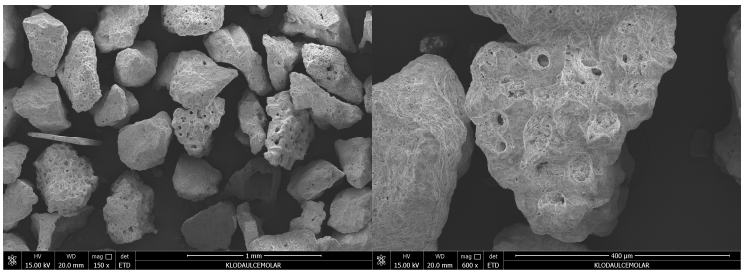

X 150 X 600

(**a**)

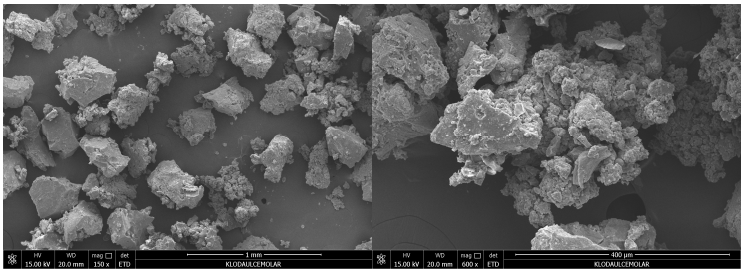

X 150 X 600

(**b**)

Figure 1. Micro-scale image of the test materials: (**a**) Calcareous sand; (**b**) rubber chips.

The general procedure of the 1-D compression test followed the British Standard (BS 1377) [24]. In contrast, as there are no specified procedures for the resonant column test, we performed the test in accordance with the way prescribed in the literature [25,26]. In the compression test, a modified oedometric compaction cell was use, i.e., a 27.6 mm diameter cell that is 30 mm high, which can apply a maximum vertical load of 16 MPa (Figure 2a). At each loading step, the settlement of the specimens was monitored so that the final void ratio could be calculated. The Stokoe-type resonant column apparatus used in this study was of bottom-fixed and top-free configuration (Figure 2b), which can accommodate a soil specimen of 50 mm in diameter and 100 mm in height. Isotropic confining pressures were applied to the specimens in a stepwise manner as 100, 200, 300, and 400 kPa. This was then followed by the resonant column test. By sweeping a sinusoid signal with a desired amplitude, the soil specimen was forced to vibrate, and the response of the specimen was recorded. Note that the strain level involved in the resonant column test was in the order of 10^{-5} or below; accordingly, the small strain shear modulus (G_0) of the specimen was determined. Those interested in more detailed information can refer to Yang and Liu [26] and Liu et al. [27] for more features about the resonant column technique.

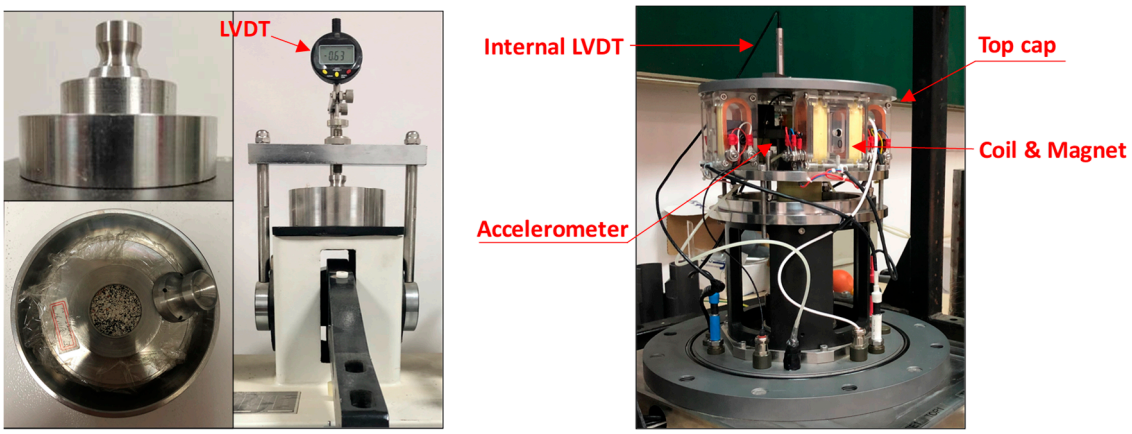

Figure 2. Test equipment: (**a**) Modified oedometer cell; (**b**) resonant column apparatus (LVDT: linear variable differential transformer).

3. Test Results and Discussion

3.1. Compression Properties

Figure 3 presents the results obtained for the rubber–sieved calcareous sand mixtures of different rubber contents and initial void ratios. Note that all of the mixtures were prepared at quite large initial void ratios, primarily since the admixture of rubber chips quickly rebounded after tamping and maintained a loose packing state.

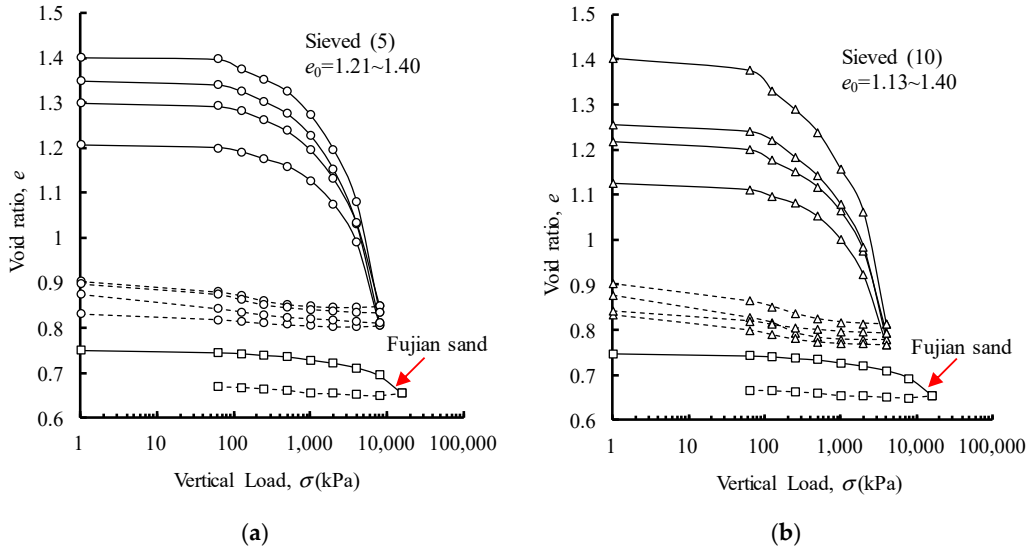

Figure 3. Compression curves of mixtures: (**a**) Rubber content = 5%; (**b**) rubber content = 10%.

Despite different initial void ratios, the virgin compression curves were originally linear and flat, indicating an elastic response. When the applied vertical load was beyond the yield stress of the mixtures, it is interesting to see that the curves tended to converge in the stress range investigated, with an implication that all specimens were compressed to a unique state not associated with the initial conditions. For comparison purposes, the compression curve of Fujian sand (Chinese standard sand) was also plotted in this Figure. It is clear that the compression curve of the Fujian sand is less steep than that of the rubber–calcareous sand mixtures, whilst the rebound curves of the test specimens are nearly parallel. The above observations strongly suggest that, under otherwise similar

conditions, rubber–calcareous sand mixtures are more compressible than Fujian sand, and that most of the deformation of the mixtures is unrecoverable during unloading. This implies that the particles were subjected to strong reorientation during loading, while during unloading, the interlocking of particles prevailed in the present cases of the mixtures with rubber chips.

Furthermore, in Figure 4, a comparison of the compression curves of specimens with different rubber contents is provided. It is noteworthy that the state where the compression curve tended to merge depended on the rubber content. More specifically, examination of the compression curves shows that the specimens of a 10% rubber content merged at a vertical load of approximately 4 MPa, whereas the specimens of a 5% rubber content merged at 8 MPa. Given the limit range of deformation in the oedometer test, the final void ratio of all tests was approximately 0.8. The observations in Figure 4 imply that the role of rubber chips of varying contents that contributed to the compressibility of the mixture was different. More specifically, when the applied load was higher than the yield stress, both the rubber particles and the calcareous sand were members of force chains. The mixture with a higher rubber content tended to have softer particles in the force chain, and it was easy to buckle under the external load. Accordingly, under the same stress level, the specimen with higher rubber content—i.e., sieved (10)—yielded a larger deformation.

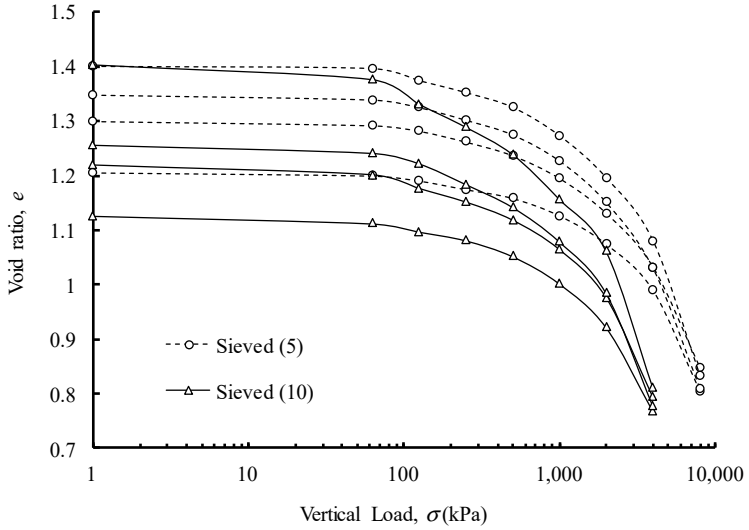

Figure 4. Comparison of the compression curves for mixtures with different rubber contents.

3.2. Grain Breakage

Bearing in mind that the calcareous sand is susceptible to being crushed under compression loads, it is interesting to consider whether the presence of rubber chips affects the crushability of calcareous sand. To address this issue, the grain crushing needs evaluating by adopting a quantitative approach, for example, using the grain crushing index. Among a list of indices, a parameter proposed by Hardin [28], namely, the relative breakage (B_r), appears to be more versatile and is often referred to in other research [10,29]. The above index is derived based on changes in the cumulative distribution of grains before and after the test and it can be simply expressed as in Equation (4):

$$B_r = B_t/B_p \tag{4}$$

where B_t is the total breakage represented by the area between the initial grading curve of sand and the final one, and B_p is represented by the area between the vertical line of d = 74 μm and the initial grading curve.

The particle size distribution curves of the test materials are presented in a semi-logarithmic format in Figure 5. It needs to be clarified that each test specimen was sieved by hand three times,

and the average values were adopted to determine the particle size distribution curves. This was not because of large discrepancies in each sieving test; rather, little difference was found in terms of the grading curves for the same mixture, implying that the potential problem of particle breakage during sieving was negligible. Hence, the shift of the distribution curves was due to the grain breakage in the compression test. Moreover, it needs to be clarified that the overall particle size of the calcareous sands after the compression test was in a range greater than 2 μm. Hence, no cohesive soils (i.e., a particle size less than 2 μm) were obtained.

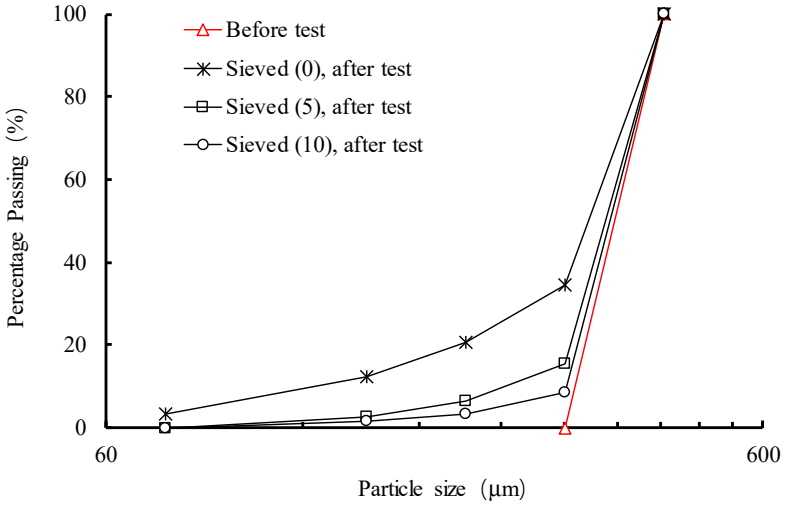

Figure 5. Particle size distribution curves of the test materials before and after the compression tests.

In Figure 6, the B_r value of the mixtures with different rubber contents were compared, along with the results of the Fujian sand. A clear difference between the Fujian sand and the calcareous sand was observed. More interestingly, a marked trend was found in that the B_r value tended to decrease with the rubber content. For example, the B_r value of the specimen with a 10% rubber content reduced by approximately 77% as compared with the pure calcareous sand—i.e., sieved (0). Moreover, little difference in the B_r value was found between the Fujian sand and the mixture with a 10% rubber content. Considering that the compressibility of the soils measured in the oedometer cell resulted from the deformation and possible reorientation of the grains, the above observations in Figures 3–6 provide solid evidence that a part of the external loads was shared by the soft plastic interparticle contacts between the rubber and the calcareous sand in the mixtures. As a consequence, the deformation of calcareous sands under external loads was well reduced.

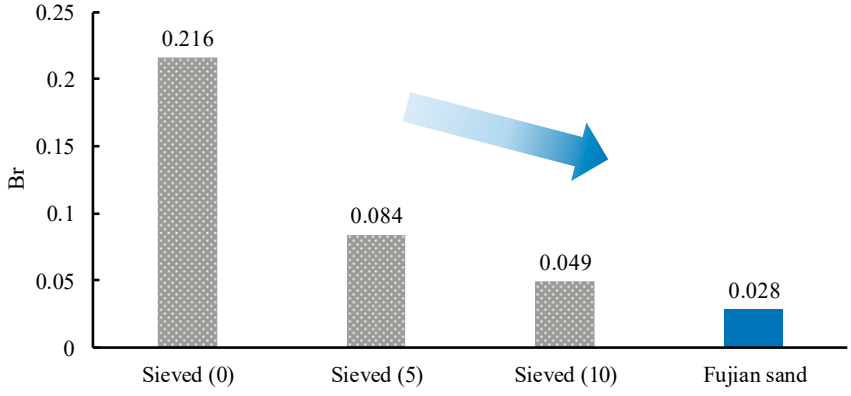

Figure 6. Breakage index of the rubber–calcareous sand mixtures and the Fujian sand.

3.3. Small Strain Modulus and Modulus Reduction

In light of the high damping and energy absorbing characteristics of the rubber chips [30,31], from an engineering perspective, understanding of the dynamic properties of rubber–calcareous sand mixtures is also important. In Figure 7, the small strain shear modulus (G_0) of the mixtures determined from the resonant column test are presented. To facilitate the comparison, the initial void ratios of the specimens remained very close (e_0 = 1.37~1.39). It can be seen in this plot that, under otherwise similar conditions, a reduction of the G_0 values was obtained for the specimens with higher rubber contents. Moreover, the trend between the effective confining pressure and the G_0 value can be characterized using a power relationship, such as $G_0 = A\ (\sigma')^n$. The reduction of G_0 was mainly reflected by the coefficient A in the way that it decreased with increasing rubber content. More specifically, the A value decreased by approximately 55% with a 10% rubber content. Accordingly, the coefficient n was stress-dependent and it increased with the rubber content. Although the G_0 gradually decreased with the add-in rubber chips, the reduction was less remarkable when the rubber content was beyond 5%. For instance, at σ' = 100 kPa, the difference in G_0 value was approximately 20 kPa between the specimens of sieved (0) and sieved (5), whereas further reduction of the G_0 value was only 12 kPa for the specimen with a 10% rubber content.

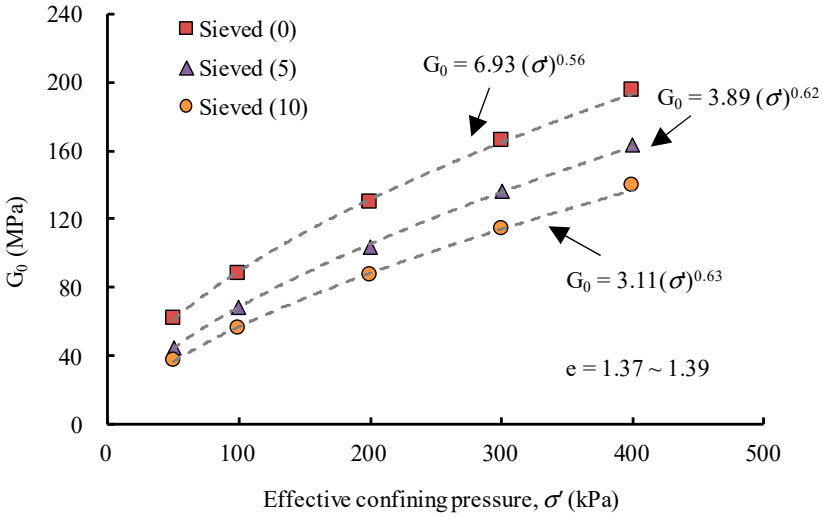

Figure 7. Small strain shear modulus (G_0) of the rubber–calcareous sand mixtures.

Moreover, the modulus reduction curves and the associated damping curves of the specimens at σ' = 200 kPa are presented in Figures 8 and 9, respectively, along with the literature values of the Fujian sand [32]. As a matter of fact, the ground response analysis during earthquakes depends on an accurate estimation of the soil modulus and damping properties at working strain (in the order of 10^{-3} or greater) [33,34]. Nevertheless, it is impractical to conduct a field test with this high level of ground shaking. Hence, the normalized modulus reduction curve and the damping curve are often used in design. Providing a small strain shear stiffness of soil (G_0), the shear stiffness (G) at any given shear strain level can be estimated. Unlike the observed discrepancies in Figure 7, little difference for the specimens of varying rubber contents can be found in Figure 8. However, the modulus reduction curves of the rubber–calcareous sand mixtures are steeper than that of the Fujian sand. Accordingly, in Figure 9, the damping curves of the mixtures appear to locate above that of the Fujian sand. Again, no significant difference was yielded by varying the rubber content.

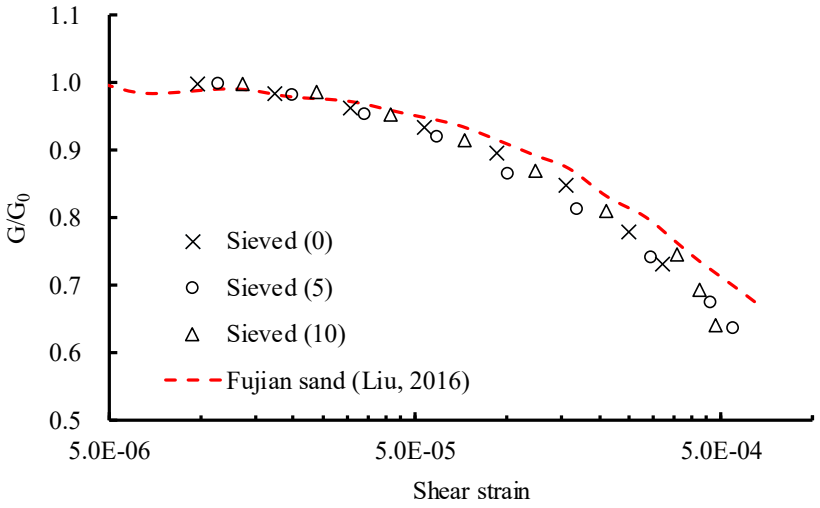

Figure 8. Modulus reduction curves of the rubber–calcareous sand mixtures.

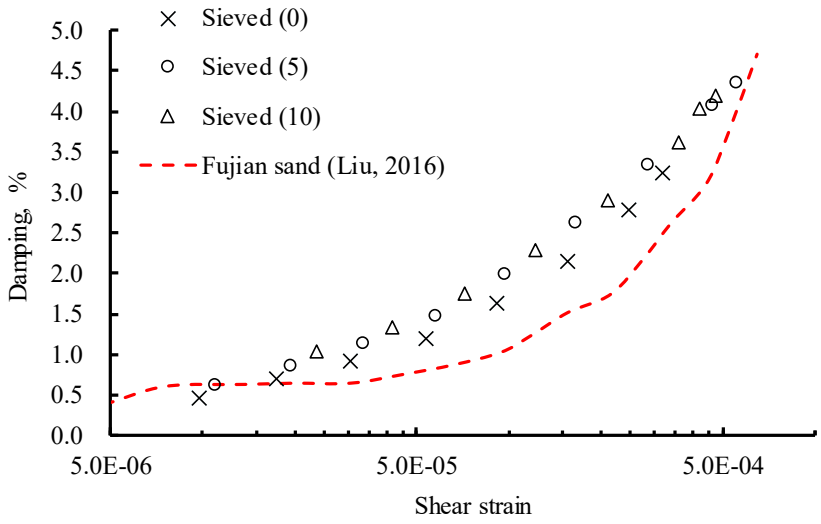

Figure 9. Damping curves of the rubber–calcareous sand mixtures.

In the above context, although the inclusion of rubber chips lowered the shear stiffness of the calcareous sand (e.g., at 400 kPa, the small strain shear stiffness of calcareous sand decreased by approximately 63% with a 10% rubber content), it is clear that the most detrimental impact of grain crushing on the calcareous sand was well minimized. In the current state of practice, on the other hand, the soil stiffness can be reinforced and improved by using a geomembrane or geogrid [8]. Of course, further studies along this line are worthwhile.

4. Conclusions

This paper presented how the addition of rubber particles alters the mechanical properties of calcareous sand through well-controlled laboratory experiments. The main findings resulting from the study are summarized as follows:

(a) The virgin compression curves of the rubber–calcareous sand mixtures tended to converge in the stress range investigated. This implies that all specimens were compressed to a unique state not associated with the initial conditions. However, the results also show that the location of the converging point depends on the rubber content.

(b) The grain crushing of the mixtures was evaluated using a parameter of relative breakage (B_r). While the B_r value of the pure calcareous sand was significantly greater than that of the Fujian sand, it reduced pronouncedly with the inclusion of rubber chips. At a rubber content of 10%, the B_r value of the mixtures was very similar to that of the Fujian sand.

(c) The small strain shear modulus (G_0) decreased for the specimens with add-in rubber chips. Moreover, the modulus reduction and damping curves exhibited little difference for the specimens of varying rubber contents. Although the inclusion of rubber chips lowered the shear stiffness of the calcareous sand, it is still considered a useful building material since it can mitigate the adverse impact of grain crushing. The shear stiffness of the mixtures could be reinforced and further improved by using a geomembrane or geogrid.

Author Contributions: Conceptualization, X.L.; methodology, X.L.; investigation, C.T.; writing—original draft preparation, X.L.; writing—review and editing, H.L.; project administration, X.L. and H.L.; funding acquisition, X.L. and H.L. All authors have read and agreed to the published version of the manuscript.

Funding: This research was funded by the National Natural Science Foundation of China, China (No. 41807226; 41927806; 41790443; 41941019); the Fundamental Research Funds for the Central Universities through Chang'an University, China (No. 300102260201); the Second Tibetan Plateau Scientific Expedition and Research program (No. 2019QZKK0905); the "111" Center, program of the Ministry of Education of China, China (No. B18046). These financial supports are gratefully acknowledged.

Conflicts of Interest: The authors declare no conflict of interest.

References

1. Ackleson, S.; Moses, W.; Montes, M. Remote sensing of coral reefs: Uncertainty in the detection of benthic cover, depth, and water constituents imposed by sensor noise. *Appl. Sci.* **2018**, *8*, 2691. [CrossRef]
2. Al-Douri, R.H.; Poulos, H.G. Cyclic behaviour of pile groups in calcareous sediments. *Soils Found.* **1994**, *34*, 49–59. [CrossRef]
3. Wang, X.Z.; Jiao, Y.Y.; Wang, R.; Hu, M.J.; Meng, Q.S.; Tan, F.Y. Engineering characteristics of the calcareous sand in Nansha islands, South China Sea. *Eng. Geol.* **2011**, *120*, 40–47. [CrossRef]
4. Giretti, D.; Been, K.; Fioravante, V.; Dickenson, S. CPT calibration and analysis for a carbonate sand. *Géotechnique* **2018**, *68*, 345–357. [CrossRef]
5. Wang, X.; Cui, J.; Wu, Y.; Zhu, C.; Wang, X.Z. Mechanical properties of calcareous silts in a hydraulic fill island-reef. *Mar. Georesour. Geotechnol.* **2020**, *38*, 1–14. [CrossRef]
6. Lan, H.X.; Zhao, X.X.; Wu, Y.M.; Li, L.P. Settlement and deformation characteristics of calcareous island-reef. *J. Ocean Univ. China* **2017**, *47*, 1–8.
7. Lv, Y.; Liu, J.; Xiong, Z. One-dimensional dynamic compressive behavior of dry calcareous sand at high strain rates. *J. Rock. Mech. Geotech. Eng.* **2019**, *11*, 192–201. [CrossRef]
8. Wei, H.; Zhao, T.; Meng, Q.; Wang, X.; He, J. Experimental evaluation of the shear behavior of fiber-reinforced calcareous sands. *Int. J. Geomech.* **2018**, *18*, 04018175. [CrossRef]
9. Donohue, S.; O'Sullivan, C.; Long, M. Particle breakage during cyclic triaxial loading of a carbonate sand. *Géotechnique* **2009**, *59*, 477–482. [CrossRef]
10. Xiao, Y.; Desai, C.S.; Daouadji, A.; Stuedlein, A.W.; Liu, H.L.; Abuel-Naga, H. Grain crushing in geoscience materials–key issues on crushing response, measurement and modeling: Review and preface. *Geosci. Front.* **2020**, *59*, 363–374. [CrossRef]
11. Liu, H.S.; Mead, J.L.; Stacer, R.G. Environmental effects of recycled rubber in light-fill applications. *Rubber Chem. Technol.* **2000**, *73*, 551–564. [CrossRef]
12. Liu, L.; Cai, G.; Liu, S. Compression properties and micro-mechanisms of rubber-sand particle mixtures considering grain breakage. *Constr. Build. Mater.* **2018**, *187*, 1061–1072. [CrossRef]
13. Deng, A.; Feng, J.R. Experimental study on sand-shredded tire lightweight fills. *J. Build. Mater.* **2010**, *13*, 116–120.
14. Lee, J.H.; Salgado, R.; Bernal, A.; Lovell, C.W. Shredded tires and rubber-sand as lightweight backfill. *J. Geotech. Geoenviron. Eng.* **1999**, *125*, 132–141. [CrossRef]

15. Zheng, Y.F.; Sutter, K.G. Dynamic properties of granulated rubber/sand mixtures. *Geotech. Test. J.* **2000**, *23*, 338–344.
16. Falborski, T.; Jankowski, R. Experimental study on effectiveness of a prototype seismic isolation system made of polymeric bearings. *Appl. Sci.* **2017**, *7*, 808. [CrossRef]
17. Lee, C.; Truong, Q.H.; Lee, W.; Lee, J.S. Characteristics of rubber-sand particle mixtures according to size ratio. *J. Mater. Civ. Eng.* **2010**, *22*, 323–331. [CrossRef]
18. Lopera Perez, J.C.; Kwok, C.Y.; Senetakis, K. Effect of rubber size on the behaviour of sand-rubber mixtures: A numerical investigation. *Comput. Geotech.* **2016**, *80*, 199–214. [CrossRef]
19. Liu, X.; Yang, J. Influence of size disparity on small-strain shear modulus of sand-fines mixtures. *Soil Dyn. Earthq. Eng.* **2018**, *115*, 217–224. [CrossRef]
20. Lan, H.X.; Chen, J.H.; Macciotta, R. Universal confined tensile strength of intact rock. *Sci. Rep.* **2019**, *9*, 6170. [CrossRef]
21. Dullien, F.A. *Porous Media: Fluid Transport and Pore Structure*; Academic Press: Cambridge, MA, USA, 2012.
22. Liu, X.; Yang, J. Shear wave velocity in sand: Effect of grain shape. *Géotechnique* **2018**, *68*, 742–748. [CrossRef]
23. Guida, G.; Sebastiani, D.; Casini, F.; Miliziano, S. Grain morphology and strength dilatancy of sands. *Geotech. Lett.* **2019**, *9*, 245–253. [CrossRef]
24. British Standard Institute (BSI). *Methods of Test for Soils for Civil Engineering Purpose*; BS1377; British Standard Institute: London, UK, 1990.
25. Liu, X.; Yang, J.; Wang, G.H.; Chen, L.Z. Small-strain shear modulus of volcanic granular soil: An experimental investigation. *Soil Dyn. Earthq. Eng.* **2016**, *86*, 15–24. [CrossRef]
26. Yang, J.; Liu, X. Shear wave velocity and stiffness of sand: The role of non-plastic fines. *Géotechnique* **2016**, *66*, 1–15. [CrossRef]
27. Liu, X.; Zhang, N.; Lan, H.X. Effects of sand and water contents on the small-strain shear modulus of loess. *Eng. Geol.* **2019**, *260*, 105–202. [CrossRef]
28. Hardin, B.O. Crushing of Soil Particles. *J. Geotech. Eng.* **1985**, *111*, 1177–1192. [CrossRef]
29. Peng, Y.; Ding, X.; Xiao, Y.; Deng, X.; Deng, W. Detailed amount of particle breakage in non-uniformly graded sands under one-dimensional compression. *Can. Geotech. J.* **2020**, *57*, 1239–1246. [CrossRef]
30. Han, L.; Wei, H.; Wang, F. Study on the vibration isolation performance of composite subgrade structure in seasonal frozen regions. *Appl. Sci.* **2020**, *10*, 3597. [CrossRef]
31. Liu, H.; Luo, G.; Gong, Y.; Wei, H. Mechanical properties, permeability, and freeze–thaw resistance of pervious concrete modified by waste crumb rubbers. *Appl. Sci.* **2018**, *8*, 1843. [CrossRef]
32. Liu, X. Laboratory Investigation of Dynamic Properties of Sand with Fines. Ph.D. Thesis, The University of Hong Kong, Hong Kong, China, 2016.
33. Ishihara, K. *Soil Behaviour in Earthquake Geotechnics*; Oxford Science Publications: Oxford, UK, 1996.
34. Liu, X.; Qin, H.; Lan, H.X. On the relationship between soil strength and wave velocities of sandy loess subjected to freeze-thaw cycling. *Soil Dyn. Earthq. Eng.* **2020**, *136*, 106216. [CrossRef]